

# Optical Shock-Enhanced Self-Photon Acceleration

P. Franke,<sup>1,2</sup> D. Ramsey,<sup>1,2</sup> T. T. Simpson,<sup>1,2</sup> D. Turnbull,<sup>1</sup> D. H. Froula,<sup>1,2</sup> and J. P. Palastro<sup>1,3,4</sup>

<sup>1</sup>Laboratory for Laser Energetics, University of Rochester

<sup>2</sup>Department of Physics and Astronomy, University of Rochester

<sup>3</sup>Department of Mechanical Engineering, University of Rochester

<sup>4</sup>Institute of Optics, University of Rochester

Photon accelerators can spectrally broaden laser pulses with high efficiency in moving electron density gradients driven in a rapidly ionizing plasma. When driven by a conventional laser pulse, the group-velocity walk-off experienced by the accelerated photons and deterioration of the gradient from diffraction and plasma-refraction limit the extent of spectral broadening. Here we show that a laser pulse with a shaped space–time and transverse intensity profile overcomes these limitations by creating a guiding density profile at a tunable velocity. Self-photon acceleration in this profile leads to dramatic spectral broadening and intensity steepening, forming an optical shock that further enhances the rate of spectral broadening. In this new regime, multi-octave spectra extending from 400-nm to 60-nm wavelengths, which support near-transform-limited <400-as pulses, are generated over <100  $\mu\text{m}$  of interaction length.

Broadband sources of coherent radiation find utility across diverse scientific disciplines as experimental drivers and diagnostic tools. State-of-the-art supercontinuum sources, which primarily achieve spectral broadening through Kerr-induced self-phase modulation of ultrashort laser pulses in either gas-filled fibers<sup>1</sup> or self-guided filaments,<sup>2</sup> routinely generate multi-octave spectra in the infrared (IR) to ultraviolet (UV) wavelength range (15  $\mu\text{m}$  to 100 nm).<sup>3–7</sup> Such sources have thus far been limited to wavelengths >100 nm, due to a lack of dispersion control and strong absorption in the extreme ultraviolet (XUV) ( $\lambda = 10$  nm to 100 nm). Extending coherent broadband sources into the extreme ultraviolet would open new wavelength regimes for spectroscopy and increase the achievable spatial and temporal resolution for applications including single-shot spectral interferometry,<sup>8</sup> transient spectroscopy,<sup>9</sup> and coherence tomography.<sup>10</sup>

Photon accelerators can spectrally broaden laser pulses with high efficiency in moving electron density gradients.<sup>11,12</sup> When driven by a conventional laser pulse, the group velocity walk-off experienced by the accelerated photons and deterioration of the gradient from diffraction and refraction limit the extent of spectral broadening [Figs. 1(a) and 2(f)],<sup>13–16</sup> Here we introduce a scheme [Fig. 1(b)] that largely eliminates the adverse effects of diffraction, refraction, and dephasing by combining spatiotemporal<sup>17–20</sup> and transverse intensity profile shaping of the laser pulse.<sup>21–23</sup> This structured flying-focus (SFF) pulse drives a guiding plasma density profile that moves at a tunable focal velocity  $v_f$ . When a properly designed SFF pulse propagates in a homogeneous, partially ionized plasma, it undergoes extreme self-steepening and spectral broadening, culminating in the formation and collapse of an optical shock.

From 2-D finite-difference time-domain simulations, we discover that this novel self-shocked photon acceleration can produce multi-octave spectra extending well into the XUV (400 nm to 60 nm) over <100  $\mu\text{m}$  of interaction length. The incident pulse had a central wavelength of 400 nm, a total energy of 53  $\mu\text{J}$ , and a total duration of 12 fs, values compatible with a tabletop Ti:Sa laser system. The intensity peak produced by the spatiotemporal shaping had a duration of 3.3 fs. The incident pulse was compressed considerably during the interaction, such that an isolated 700-as pulse was obtained at the accelerator output (90- $\mu\text{m}$  interaction length). A simple short-pass filter can isolate even shorter 1.3 $\times$  transform limited, highly focusable, coherent, high-intensity

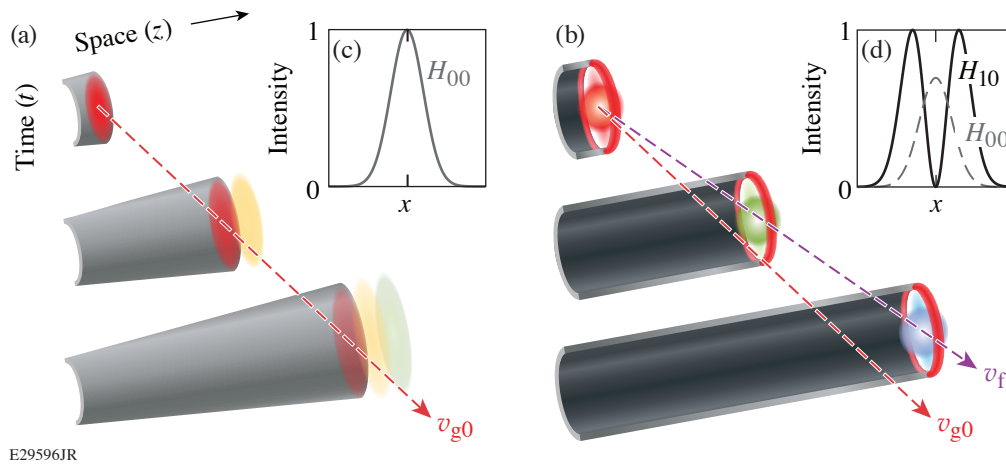


Figure 1

(a) A Gaussian beam drives a (gray) radially convex ionization front at the group velocity of light over approximately a Rayleigh length. Photons diverge from the optical axis due to diffraction and plasma refraction. Frequency upshifted photons dephase from the ionization front due to group velocity walk-off, limiting the system to relatively small frequency shifts. (b) A SFF pulse drives a concave ionization front at a tunable focal velocity  $v_f \gtrsim v_{g0}$  over a distance much greater than a Rayleigh length. Photons are concentrated near the optical axis and stay in phase with the ionization front, resulting in many photons undergoing a large frequency shift. Transverse intensity profiles of a typical (c) Gaussian pulse and (d) SFF pulse used in 2-D simulations. Spatiotemporal shaping causes the intensity peak of the SFF to propagate at a tunable velocity in the far field. The guiding-transverse profile is achieved by combining orthogonally polarized Laguerre-Gaussian spatial modes.

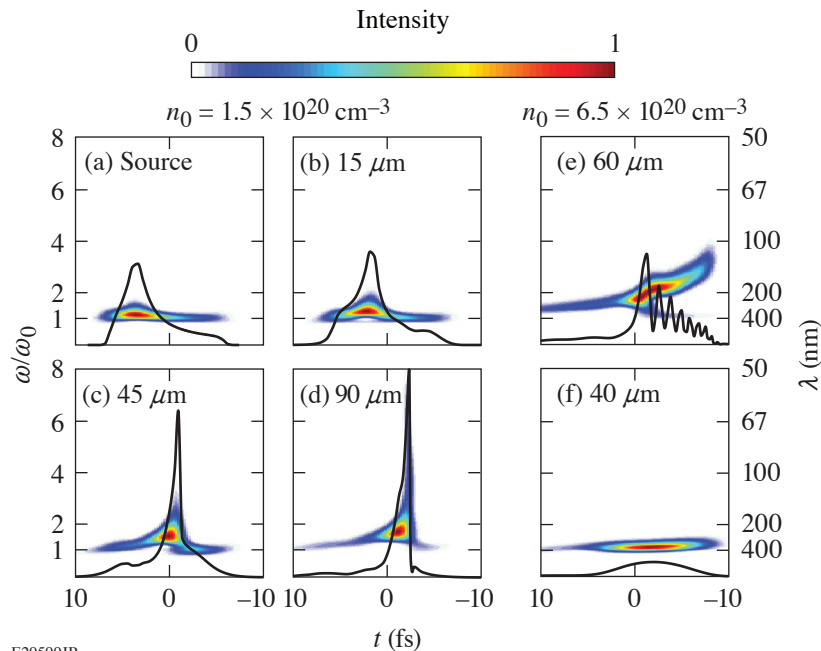


Figure 2

Spectrograms obtained by wavelet transform of the electric field on the optical axis for a SFF pulse at (a) the source input plane, (b)  $15 \mu\text{m}$ , (c)  $45 \mu\text{m}$ , and (d)  $90 \mu\text{m}$ , with  $v_f = 1.015 v_{g0} = 0.9817 c$ , and an initial neutral density  $n_0 = 1.5 \times 10^{20} \text{cm}^{-3}$ . For comparison, the spectrograms at higher density ( $n_0 = 6.5 \times 10^{20} \text{cm}^{-3}$ ) are shown for (e) a SFF pulse with  $v_f = 1.030 v_{g0} = 0.8740 c$ , and (f) a standard Gaussian pulse focused at  $z = 10 \mu\text{m}$ . The color scale in each plot is normalized to the peak intensity. On-axis intensity profiles (black) are normalized to  $10^{17} \text{W/cm}^2$ .

( $>10^{15} \text{W/cm}^2$ ), subfemtosecond pulses (350 as,  $9\times$  temporal compression) from the accelerator output without the need for post compression. Spectral filtering could be achieved by allowing the output pulse to naturally diffract out of the end of the accelerator, collimating it with an appropriate curved reflector,<sup>24</sup> and then allowing it to pass through a 200-nm-thick magnesium foil.<sup>25</sup> The filtered pulse could then be refocused on target using another curved reflector.

Spatiotemporal shaping produces a focal region much longer than a Rayleigh length and allows the peak laser intensity to move through the accelerator at a velocity  $v_{g0} < v_f < c$ , where  $v_{g0}$  is the initial group velocity of the pulse. Under these condi-

tions, the intensity peak moves forward within the pulse's temporal envelope, such that self-accelerated photons at the back of the pulse catch up to and remain in phase with the intensity peak formed by the unshifted photons as they come into focus. The transverse intensity profile of the pulse has higher off-axis intensity. The resulting optical field ionization creates a guiding, radial electron density gradient that dynamically forms just ahead of the central axial density gradient responsible for the photon acceleration. Accelerated photons, thus confined near the optical axis, overlap temporally and spatially with other photons of varying frequency. This local increase in bandwidth and photon density leads to dramatic self-steepening and elevated amplitude of the main intensity peak. The resulting sharpened axial gradient causes faster frequency shifting and more sharpening, which in turn causes even faster frequency shifting [Figs. 2(a)–2(d)]. Eventually, optical wave breaking terminates the self-steepening and limits the maximum extent of spectral broadening. Increasing the initial density of the target increases the group-velocity dispersion, leading to shorter wave-breaking distances and smaller maximum frequency shifts [Fig. 2(e)].

The unique combination of compact size, short wavelength, broad bandwidth, and high coherence distinguishes this approach from other currently available sources. An experimental realization would provide a novel tabletop source of coherent broadband radiation and attosecond pulses in the XUV that could eventually scale to a tabletop source of coherent soft x rays. Democratizing access to extreme light through the development of radiation sources, such as that described here, could lead to an increased rate of scientific progress across fields that have far-reaching and positive impacts in fields such as material science, biology, and clean energy.

This material is based upon work supported by the Office of Fusion Energy Sciences under Award Number DE-SC0019135, the Department of Energy National Nuclear Security Administration under Award Number DE-NA0003856, the University of Rochester, and the New York State Energy Research and Development Authority.

1. J. M. Dudley, G. Genty, and S. Coen, *Rev. Mod. Phys.* **78**, 1135 (2006).
2. A. Couairon and A. Mysyrowicz, *Phys. Rep.* **441**, 47 (2007).
3. K. Jiao *et al.*, *Opt. Lett.* **44**, 5545 (2019).
4. F. Belli *et al.*, *Optica* **2**, 292 (2015).
5. A. Ermolov *et al.*, *Phys. Rev. A* **92**, 033821 (2015).
6. J. C. Travers *et al.*, *Nat. Photon.* **13**, 547 (2019).
7. N. Aközbebek *et al.*, *New J. Phys.* **8**, 177 (2006).
8. H. Mashiko *et al.*, *Opt. Express* **28**, 21025 (2020).
9. K. Ramasesha, S. R. Leone, and D. M. Neumark, *Annu. Rev. Phys. Chem.* **67**, 41 (2016).
10. F. Wiesner *et al.*, *Optica* **8**, 230 (2021).
11. S. C. Wilks *et al.*, *Phys. Rev. Lett.* **62**, 2600 (1989).
12. J. T. Mendonça, *Theory of Photon Acceleration*, Series in Plasma Physics (Institute of Physics Publishing, Bristol, England, 2001).
13. J. M. Dias *et al.*, *Phys. Rev. E* **66**, 056406 (2002).
14. N. C. Lopes *et al.*, *Europhys. Lett.* **66**, 371 (2004).
15. J. M. Dias *et al.*, *Phys. Rev. Lett.* **78**, 4773 (1997).
16. A. Howard *et al.*, *Phys. Rev. Lett.* **123**, 124801 (2019).
17. D. H. Froula *et al.*, *Nat. Photonics* **12**, 262 (2018).
18. A. Sainte-Marie, O. Gobert, and F. Quéré, *Optica* **4**, 1298 (2017).
19. J. P. Palastro *et al.*, *Phys. Rev. Lett.* **124**, 134802 (2020).
20. T. T. Simpson *et al.*, *Opt. Express* **28**, 38516 (2020).
21. M. W. Beijersbergen *et al.*, *Opt. Commun.* **112**, 321 (1994).
22. Y. Shen *et al.*, *Light Sci. Appl.* **8**, 90 (2019).
23. A. Longman *et al.*, *Opt. Lett.* **45**, 2187 (2020).
24. C. Bourassin-Bouchet *et al.*, *Opt. Express* **21**, 2506 (2013).
25. G. D. Tsakiris *et al.*, *New J. Phys.* **8**, 19 (2006).